Synchronous vs asynchronous diffusion–reaction processes involving geminate radical pairs

3 AUTHORS, INCLUDING:

E. Abad
Universidad de Extremadura
44 PUBLICATIONS **256** CITATIONS

Synchronous vs asynchronous diffusion–reaction processes involving geminate radical pairs

Kristopher G. Urie [a,1], John J. Kozak [a], E. Abad [b,*]

[a] *DePaul University, 243 South Wabash Avenue, Chicago, IL 60604-2301, United States*
[b] *Departamento de Física, Universidad de Extremadura, E-06071 Badajoz, Spain*

ARTICLE INFO

ABSTRACT

We report lattice Monte Carlo calculations to study the efficiency of diffusion-controlled reactive processes involving geminate radical pairs. Whereas our earlier study [J.J. Kozak, C. Nicolis, G. Nicolis, N.J. Turro, J. Phys. Chem. 105 (2001) 10949] focused on factors affecting the reaction efficiency when a pair of coreactants moved synchronously on a surface modeled as a $d = 2$ dimensional square planar lattice subject to periodic boundary conditions, we document here differences in reaction efficiency when a pair of coreactants can move synchronously *or* asynchronously on surfaces which are topologically different but characterized by the same number N of sites. As before, the first surface is taken to be a $d = 2$ square planar lattice; the second surface considered is a Cartesian shell, the bounded surface of a cube. When studied as a function of system size, we find that synchronous dynamics are more efficient than asynchronous dynamics in optimizing diffusion–reaction processes; and, reactions on planar, periodic surfaces are more efficient than on cubic shells. The relevance of these conclusions to experimental studies on two radiation-induced, radical decay reactions [the one cited above and A.J. Frank, M. Grätzel, J.J. Kozak, J. Am. Chem. Soc. 98 (1976) 3317] is noted and discussed.

© 2010 Elsevier B.V. All rights reserved.

1. Introduction

Two earlier reports [1,2] provide the motivation for the present study. The first was an experimental study of radical decay kinetics facilitated by a micellar system [1]. The dismutation reaction of Br_2^- ion radicals in aqueous solution in the presence of micellar cetyltrimethylammonium bromide (CTAB) was studied by a pulse radiolysis technique. Analysis of the kinetic data, complemented by calculations based on a lattice model, showed that the kinetics could be understood in terms of the concept of *reduction of dimensionality* [3]. The second report was an analytical and computational study of photochemical reactions involving molecules such as 1, 3-diphenyl acetone [2]. This study focused on quantifying the efficiency of diffusion–reaction processes involving geminate radical pairs moving synchronously (or not) on the surface of a catalyst (e.g. a zeolite) support.

In the studies carried out in Refs. [1,2], discrete-time lattice models were used to obtain theoretical estimates for the relevant experimental quantities (e.g. ratios of kinetic constants). These lattice-statistical models have the advantage of providing a straightforward way of modeling the occurrence of different, simultaneously-active channels, e.g. reactive collisions via same-site occupancy and position exchange of two reactants during a single time step. Although an approach based on a stochastic, continuous-time random walk (CTRW) model can be formulated (see Section 2), in this study we

---

* Corresponding author.
  E-mail address: enrique.abad@bioch.ox.ac.uk (E. Abad).

[1] Present address: Field Museum of Natural History, 1400 S. Lake Shore Dr., Chicago, IL 60605-2496, United States.

augment our analysis by a simpler, continuous-time, chemical kinetic model (which, as we shall demonstrate, yields results essentially the same as those obtained using our discrete-time model).

The principal goal of the present work is to generalize the results obtained in Refs. [1,2] by re-examining the role of substrate geometry and extending the positional options available to (the update rules imposed on) the coreactants involved in the two radiation-induced radical decay reactions. To provide a common setting within which both decay reactions can be considered, we represent each substrate (micellar surface, zeolite surface) using a lattice model, and then study the kinetic consequences as a function of different lattice characteristics (e.g., Euler characteristic, system size). Further, we shall consider different transition scenarios, i.e., one in which one reactant is stationary and the second moves randomly at each time step (the asynchronous case) and a second scenario where both coreactants can move simultaneously (the synchronous case).

The primary difficulty in treating the synchronous case is that one must take into account additional interaction channels which become available when particles interchange their positions (These difficulties are bypassed in continuum approaches to similar problems, where analytic results have been presented in several noteworthy studies [4–9]). In contrast to the asynchronous case, for which the classic results of Montroll [10] are available to guide one's work, only recently has the study of synchronous motion using the theory of finite Markov processes yielded exact (numerical) results [11–13]. In light of this development, it is of interest to revisit the problems considered in Refs. [1,2] and to explore whether a more robust theoretical treatment of the two experimental problems addressed there leads to the same qualitative/quantitative results—or not. Exploring this question is the motivation for the present study.

2. Kinetics of photogenerated radical pairs on a catalyst surface

2.1. Description of the experimental system and the Monte Carlo simulations

Since the relevance of the calculations reported here is more easily displayed in the study [2], we consider this work first. In most photochemical reactions, the generation of geminate radicals produces triplet pairs. A "spin flip" to a reactive singlet pair must occur before the radicals can combine; such a "spin flip" can occur through some magnetic effect in the environment acting on one or both of the spins [14–20].

Supposing there is an immobile site S at which a spin flip can occur, the recombination of the radicals $R^\uparrow = X_1$ and $R^\downarrow = X_2$ can be described by the following reaction sequence:

$$
\begin{aligned}
&X_1 + S \rightarrow X_2 + S \\
&X_2 + S \rightarrow X_1 + S \\
&X_1 + X_2 \rightarrow \text{product } (R\text{–}R) \\
&X_1 + X_1 \rightarrow X_1 + X_1 \\
&X_2 + X_2 \rightarrow X_2 + X_2.
\end{aligned}
\tag{1}
$$

Our lattice model is designed to reflect the current understanding of the experimental situation. The radicals perform random nearest-neighbor jumps at discrete time steps. The first two steps in (1) are realized only when a radical encounters site S. The third step describes the generation of products, which can take place either by same-site occupancy, or when the two reactants swap positions (long-range radical–radical interactions are neglected). The last two steps in the reaction scheme (1) take into account the experimental fact that no reaction can occur between radicals of the same spin; in our simulations, when two radicals with the same spin converge on a given lattice site, they are both reset to their previous positions.

The above scheme was studied both analytically (using the theory of finite Markov processes and via a classical kinetic model) and numerically (via Monte Carlo simulations) in Ref. [2]. The lattices chosen for the study were square planar lattices of $n \times n = N$ sites subject to periodic boundary conditions. In each displacement, the species X_1 and X_2 were assumed to move synchronously, i.e., *both X_1 and X_2 move with unit probability in the next time step*.

A host medium that can provide a template to trigger the "spin flip" of a geminate radical is the surface of a crystallite containing a magnetic ion. Since a cubic shell is a more reasonable model of such a surface, we generalize our earlier study to consider, in addition to planar lattices subject to periodic boundary conditions, diffusion–reaction processes taking place on the surface of a cube. Whereas the latter surface is (also) of topological dimension $d = 2$, it has a different Euler characteristic ($\Omega = 2$) than a periodic planar lattice ($\Omega = 0$).

In the photochemical reaction [2], X_1 and X_2 are identical except for their spin state, so there is no reason *a priori* to suppose that each will not move in a given time step, implying that X_1 and X_2 move synchronously. In a real system at finite temperature, however, thermal fluctuations can arise; moreover, the site-to-site transitions of species X_1 in the vicinity of a local, static imperfection may be different from transitions of species X_2 in a region free of defects (and vice versa). In either event, the probability P_1 of species X_1 moving and the probability P_2 of X_2 moving need not be uniformly the same for all sites on the lattice. To gain some insight into the importance of these factors, we consider the possibility that species X_1 and X_2 can move *either* synchronously *or* asynchronously.

Before continuing, a referee has noted, correctly, that the presence of localized, but randomly-distributed spatial imperfections confers on the lattice model adopted here the properties of a random medium. Methods for dealing with

transport in random media have been extensively developed [see the seminal treatise by Weiss, Ref. [21]], in particular, the CTRW model introduced by Montroll and Weiss [see Ref. [21], Chapter 2, for a pedagogical introduction to the CTRW model]. Although we restrict attention in this study to a discrete-time, Markovian analysis, we agree that an important next step in dealing with the complexities of the experimental work referenced in Ref. [2] would be to account for spatial inhomogeneities (along with variable yet finite barrier heights) by introducing memory effects via a non-Markovian analysis involving waiting time distributions. We note that CTRW models designed for homogeneous substrates have been successful in describing aspects of stochastic processes in disordered systems if suitable waiting-time distributions are imposed [Ref. [21], p. 297] (in the absence of a detailed knowledge of the disorder configuration, the usual hypothesis is to assume a random distribution of imperfections and to compute ensemble-averaged properties for comparison with experiments; see, for example, Ref. [22]). Some insight into the consequences of adopting variable (random) waiting times can be extracted from the present study since, as we shall demonstrate later, in our computation strategy for the case of asynchronous dynamics, a walker may hop/jump or "stall" at each tick of the clock, its waiting time thus becoming a stochastic variable.

To continue, our formulation allows one to distinguish between and quantify the consequences as regards reaction efficiency of two possible reaction sequences. In the first, we consider a system where a spin flip transition has *already* occurred, thus yielding a reactive pair having different spin states X_1 and X_2 (only the third step in Eq. (1) is retained). At the beginning of each "no-flip" simulation, each radical is positioned at a random site on the lattice (with the proviso that two radicals never occupy the *same* site). At each time step, each radical is allowed to move, either synchronously or asynchronously following the computational algorithm described in a later paragraph. If, at the end of a time step, both radicals occupy the same site or have swapped sites (i.e., occupy the coreactant's previous site), a recombination reaction is considered to have taken place (the third step in the reaction scheme, Eqs. (1)), and the trial (simulation) is terminated. Only nearest-neighbor displacements are considered in the present study, although this constraint can easily be relaxed in subsequent work.

The second reaction sequence considered here, the full kinetic scheme, Eqs. (1), is then studied, i.e., reactions involving a "spin flip" are taken into account. In the "flip" simulations, we restrict our attention to the case where there is a single magnetic site S on the lattice that causes the spin of a radical to change. Inasmuch as the number and distribution of such flipping sites S in a "real" system is expected to be random, the case considered represents a simplification but, again, one that could be lifted in subsequent work. For the periodic square lattice, the site S can be anywhere, as all sites are symmetry-equivalent; on the surface of a cubic shell, S is at the center of one face (for odd valued N) or at any of the four symmetry-equivalent sites located closest to the center of a face (for even-valued N). Once the position of the (single) site S is assigned, at the beginning of the trial, each radical is randomly assigned one of two possible spin values. The computational algorithm described in the following paragraph is implemented, with the caveat that if two radicals of the same spin encounter each other, the simulation is not terminated; rather, both radicals are reset to their previous positions on the lattice. If a given radical encounters the site S, its spin is switched to the opposite setting. As in the experimental situation, the site S retains its "spin-flipping" character after interaction with a given radical; thus, a radical can undergo several spin flips before encountering the other diffusing radical. Finally, if at a particular stage in the simulation, two radicals having opposite spins attempt to occupy the same site (or have swapped sites), the recombination reaction takes place and the trial is terminated.

At a more detailed level, the "rules of engagement" of two radicals at a given lattice site are these. Consider first a site which is not a "spin flip" site S. To explore the asynchronous case, we adopt the convention that the motion of the two particles X_1 and X_2 is such that the respective probabilities $[P_1, P_2]$ randomly take the values $[1, 0]$ and $[0, 1]$ on successive time steps, in contrast to the synchronous case where species X_1 and X_2 are assumed to move with unit probability at every time step, i.e., $[P_1, P_2] = [1, 1]$. For the synchronous case, the computational algorithm is straightforward; for the asynchronous case, one reactant is chosen (randomly) at a given time step, and moves (randomly) while the second reactant is held stationary. Numerous trials are necessary before reliable results are obtained (see the last paragraph of this section).

Now, consider the case where one radical is positioned on the site S. In the asynchronous case, if a radical happens to be localized at the flipping site S, its spin is flipped at every time step. If the second, diffusing radical encounters the site S at some time step and its spin happens to be opposite to that of the radical at that site, reaction takes place. Otherwise, the diffusing radical is reset at its prior site on the lattice. The synchronous case is simpler since if two radicals of *opposite* spin are simultaneously flipped, reaction (still) takes place. And, finally, if two radicals with the *same* spin are simultaneously flipped, no reaction occurs and both radicals are reset at their previous locations.

In our simulations, we determine the mean walklength (site-to-site displacements) for radicals X_1 and X_2 before an irreversible reaction takes place, first for the "no-flip" case and then for the more general situation described above. Each set of trials was ended when a 95% confidence interval of the mean displacement was less than 0.01 times the mean displacement. Different topologies and system sizes require different numbers of trials to achieve the desired precision. "Experimentally" we have found that the typical number of trials needed ranges between 40,000 and 55,000.

2.2. Numerical results and a kinetic mean field description

Displayed in Fig. 1 are the results of our Monte Carlo simulations on periodic $d = 2$ planar lattices ($\Omega = 0$) and $d = 2$ cubic shells ($\Omega = 2$). For companion lattices having the same number N of sites, the mean walklength $\langle n \rangle$ is shown both for no-flip and flip simulations.
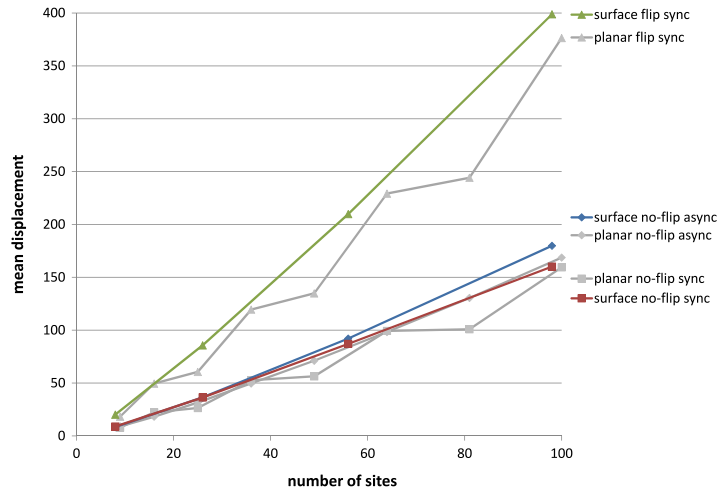
Fig. 1. Mean walklength (displacement) vs. number of lattice sites for flip and no-flip processes in both planar periodic lattices and the surface of a cube. The "no flip" curves correspond to simulations where a spin flip was assumed to have already occurred prior to monitoring the trajectory of both radicals, whereas the "flip" curves indicate that a spin transition occurs in the course of the dynamics. Both synchronous and asynchronous processes are considered. The lines between the different symbols are simply guides to the eye. The gray symbols correspond to simulations on square planar lattices, where the red, blue and green symbols correspond to simulations on cubic shells. (For interpretation of the references to colour in this figure legend and in the text, the reader is referred to the web version of this article.)

Let us first turn to the results for the no-flip case. The relative efficiency of synchronous vs. asynchronous motion on companion surfaces of N sites was studied as a function of system size. We find that on the $\Omega = 0$ planar surface, synchronous motion of X_1 and X_2 is the more efficient process (i.e., requires a fewer number of displacements of the two random walkers before reaction). On the $\Omega = 2$ cubic shell, the same ordering of reaction efficiency for synchronous vs. asynchronous motion was found to hold. A possible explanation for this difference in efficiency relies on the fact that for large enough systems the relative diffusion coefficient is larger in the synchronous case, thus facilitating particle encounter (see Ref. [11]). The walklength oscillations observed in the case of synchronous motion on the planar lattice can be ascribed to a parity effect in the number of lattice sites N, documented and discussed in an earlier work (Ref. [13]). Depending on the lattice parity and the initial positions of the radicals, only one or both of the reaction channels (same site occupation and site swapping) will be simultaneously active, thereby leading to a smaller value of $\langle n \rangle$ in the latter case.

The most important conclusion that can be drawn from Fig. 1 is that for a lattice of a given size and topology, the mean walklength in the asynchronous case is equal to or greater than the walklength in the synchronous case. That is, diffusion–reaction processes involving the *synchronous* motion of radicals are markedly *more* efficient than processes wherein the diffusion of the radicals is asynchronous.

Our calculations also document that diffusion–reaction processes on a periodic planar surface ($\Omega = 0$) are more efficient than on a $\Omega = 2$ cubic shell. An intuitive explanation of the higher efficiency of processes on a planar latttice subject to periodic boundary conditions versus processes on the surface of a (finite) cube is provided by the following argument.

Consider the particular asynchronous case where one of the radicals (say X_2) is always stationary ($P_2 = 0$) at an arbitrary site of a square planar lattice (thus playing the role of a static trapping site), and the other radical (say X_1) always moves from site to site at *each* time step ($P_1 = 1$). Assume that, after a given step, X_1 is found at a site on the boundary of a square planar lattice subject to periodic boundary conditions. In the next step the particle remains at the boundary site with probability 3/4; one out of four times it will attempt to step "out of" the lattice and be reset at the boundary site on the opposite site of the lattice (exactly at the *same* distance from the trapping site). Now consider the case where the same kinetics take place on the surface of a cube and the analogous situation where X_1 is found at an edge site, there are 3 chances out of 4 that in the next step X_1 will remain on that "face" of the cube, but one chance out of four that it will move to a site on an adjacent face. Let us suppose, for definiteness, that the trap X_2 is on the "first" face of the cube; then the consequence of stepping onto an adjacent face of the lattice will be that X_1 moves *farther away* from X_2. A similar argument can be designed for the synchronous case, only here two stages in the trial (two successive nearest-neighbor displacements of the two diffusing radicals) must be catalogued; the net result of this enumeration leads to same conclusion as noted for the asynchronous case.

Next, let us turn to the synchronous no-flip case. It is of interest to make a connection between the Monte Carlo simulations reported here, the earlier Markovian results reported in Ref. [11], and the classical, continuous-time (mean-field) kinetic analysis presented in Ref. [2]. We characterize the possible states of the system using the spin values of the radicals X_1 and X_2; in particular, we introduce the notation

$$a = [X_1, X_1], \qquad b = [X_1, X_2] \quad \text{and} \quad c = [X_2, X_2]. \tag{2}$$

In this representation, each bracket denotes a possible, joint spin state of the two radicals. In a kinetic, mean-field formulation, all spatial factors are suppressed. The state $[X_1, X_2]$ is equivalent to the state $[X_2, X_1]$ and transitions among the three states a, b and c are analyzed via the following set of kinetic equations:

$$a \quad \overset{2k}{\underset{k}{\overset{\longrightarrow}{\longleftarrow}}} \quad b \tag{3a}$$

$$c \quad \overset{2k}{\underset{k}{\overset{\longrightarrow}{\longleftarrow}}} \quad b \tag{3b}$$

$$b \overset{k'}{\longrightarrow} \text{product.} \tag{3c}$$

As we shall document shortly, the constants k and k' are related to the typical time scales (mean walklengths) for a walker to reach the immobile flipping site S and for two synchronously moving walkers to undergo a reactive collision, respectively. The weight factor "2" multiplying the kinetic rate constant k for transitions to state b arises since we regard states $[X_1, X_2]$ and $[X_2, X_1]$ as equivalent.

In the theory of finite Markov processes, the probability distribution function $\rho_n(t)$ describing the system's evolution is determined via solution of the stochastic master equation

$$\mathrm{d}\rho_n(t)/\mathrm{d}t = -\sum_{m=1}^{N} G_{nm}\rho_m(t). \tag{4}$$

Here, $\rho_n(t)$ is the probability of being in a specific, intermediate, state n at time t, with the initial condition specified to be

$$\rho_n(t = 0) = \delta_{ni}, \tag{5}$$

where i is the initial state of the system and δ is the Kronecker delta. In Eq. (4), G_{nm} is the transition rate of the probability to the state n from the state m. The **G** matrix is linked to the $N \times N$ Markov transition probability matrix **P** whose elements p_{nm} give the probability that the random walker, conditional on being in state n at time t, will be in the state m in the next step; the defining relation is

$$G_{nm} = \delta_{nm} - p_{nm}. \tag{6}$$

Moments of the distribution function $\rho_n(t)$ can be determined from Eq. (4), the *first* moment of which is the mean walklength $\langle n \rangle$. Owing to the exponential character of the formal solution to the linear equation (4), the behavior in the long-time limit is dominated by the smallest eigenvalue in the computed spectrum. This (smallest) eigenvalue is well-approximated by the inverse of the mean walklength, an equivalency which becomes exact in the limit of large system size.

The rate constants k and k' in (3) depend on the lattice geometry and are determined as follows. In order for a transition from state b to state a to occur, X_2 must reach the (stationary) magnetic site S. The average number of displacements $\langle n \rangle_{1W-T}$ needed by a walker performing nearest-neighbor jumps to reach a stationary target (reactive site) was computed exactly in Ref. [11] for several planar lattice geometries (e.g., $\langle n \rangle_{1W-T} = 9$ for a 3×3 planar lattice subject to periodic boundary conditions). As already noted, the smallest eigenvalue of the master equation associated with this stochastic process is related to the inverse of $\langle n \rangle_{1W-T}$ (a result which becomes exact in the limit of large system size). Thus, $\langle n \rangle_{1W-T}$ is a measure of the rate constant for the diffusion–reaction event; accordingly, we set $\langle n \rangle_{1W-T} = 1/k$. Similar reasoning pertains to the reverse transition, state a to state b, except that, since there are two mobile spins that can confront the site S, the rate is twice as large. The same arguments also apply to transitions between state b and state c. Note, however, that the reaction between *unlike* radicals is characterized by the mean number of steps $\langle n \rangle_{2W}$ needed for *two* walkers to collide or exchange positions. The quantity $\langle n \rangle_{2W}$ was also computed (exactly) in Ref. [11] for several square-planar lattices subject to periodic boundary conditions (e.g., $\langle n \rangle_{2W} = 8$ for a 3×3 square planar, periodic lattice). In this case, we set $\langle n \rangle_{2W} = 1/k'$.

The question then is whether and to what extent a classical, continuous-time chemical kinetic theory, one that incorporates the calculated rate constants (k, k'), can describe the system dynamics in Ref. [2] and here. The kinetic equations corresponding to the sequence, Eqs. (3) are:

$$\mathrm{d}[a]/\mathrm{d}t = -2k[a] + k[b] \tag{7a}$$
$$\mathrm{d}[b]/\mathrm{d}t = +2k[a] + 2k[c] - 2k[b] - k'[b] \tag{7b}$$
$$\mathrm{d}[c]/\mathrm{d}t = -2k[c] + k[b] \tag{7c}$$

where $[a]$, $[b]$, $[c]$ are the ensemble probabilities of the system's being in states a, b or c, respectively.

Defining the matrices

$$\begin{Vmatrix} [a] \\ [b] \\ [c] \end{Vmatrix} = \boldsymbol{S} \tag{8}$$

$$\begin{vmatrix} 2k & -k & 0 \\ -2k & (2k+k') & 2k \\ 0 & -k & 2k \end{vmatrix} = \boldsymbol{M} \tag{9}$$

the Eq. (7) can be cast into a representation structurally similar to Eq. (4),

$$(\mathrm{d}/\mathrm{d}t)\boldsymbol{S} = -\boldsymbol{MS}. \tag{10}$$

From the coefficient matrix $\boldsymbol{M}$, the following eigenvalue equation is obtained:

$$\lambda^2 - (4k + k')\lambda + 2kk' = 0. \tag{11}$$

Both roots λ of this eigenvalue equation are positive, and the one with the smallest value dominates the long-time behavior of the system. For a given λ, the decay time τ of the system to the absorbing state is given (in dimensionless units) by the identity $\lambda^{-1} = \tau$. To quantify the above for a specific geometry, consider the reaction sequence, Eqs. (3), taking place on a 3×3 lattice subject to periodic boundary conditions. Using the values $k = 1/9$, $k' = 1/8$ [see Ref. [2]], the two roots of the above eigenvalue equation are

$$\lambda_1 = 0.053878$$
$$\lambda_2 = 0.515566$$

from which one finds

$$\tau_1 = 18.560$$
$$\tau_2 = 1.940.$$

The value of τ_1 may be compared with the value of $\langle n \rangle$ determined via the Markovian and Monte Carlo approach developed in Ref. [11]; specifically,

$$\langle n \rangle = 18.818.$$

Since the mean-field description, Eq. (10), is formulated in continuous time, whereas the lattice calculations were carried out in discrete time, the agreement between the two styles of calculations is surprising. We *conjecture* that this is due to the fact that the constants (k, k') used in calculating the $\{\lambda_i\}$ incorporate the geometry of the problem as posed, leaving the time dependence to be determined via a linear differential equation, Eq. (10), structurally similar to the stochastic master equation, Eq. (4). The apparent agreement between the two styles of calculation suggests that the reaction channels that are neglected in a continuum approach (but considered explicitly in a discrete-time lattice approach) do not change the fundamental, qualitative description of the kinetic process. That there is still a difference between the two values calculated may be a consequence of the fact that in the mean-field theory of chemical reactions *all* fluctuations in the state variables are suppressed.

In accord with the experimental situation, our simulations were carried out assuming no correlations between reactant positions at time $t = 0$; the initial spin states were assigned independently for the two radicals, and independent of their positions relative to the location of the site S. In Ref. [2] we determined that photochemical generation of a triplet pair, followed by their subsequent synchronous diffusion, spin flip, and eventual recombination, lengthens the mean reaction time by a factor of ~ 2 relative to the case where X_1 and X_2 are assumed to be present at the very outset. This result is sustained in the more extensive simulations reported here. Fig. 2 displays the results for two radicals positioned initially on a $d = 2$ square-planar, periodic lattice. Comparing the curve with gray triangles in Fig. 2 with the results reported in Table 1 of Ref. [2], one finds that the two sets of results are in excellent agreement.

3. Dismutation reaction of Br_2^- radicals in the presence of micelles

3.1. Description of the system and previous results

We turn now to the study of the dismutation reaction of Br_2^- ion radicals in aqueous solution in the presence of CTAB micelles [1]. As noted earlier, one of the objectives of the present study was to analyze both radical decay reactions using a common theoretical framework. Hence, we model the micellar surface using a lattice model and perform calculations in discrete time. The relevant reactions are
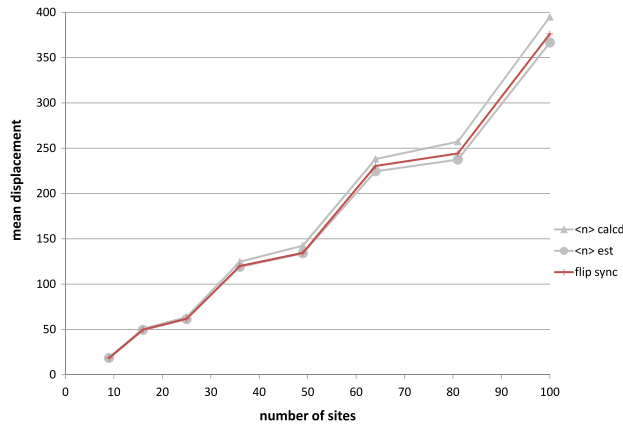
$$Br^{\cdot} + Br^- \underset{\leftarrow}{\overset{\longrightarrow}{\rightleftharpoons}} Br_2^-$$
$$Br_2^- + Br_2^- \rightarrow Br_3^- + Br^- \tag{12}$$
$$Br_3^- \underset{\leftarrow}{\overset{\longrightarrow}{\rightleftharpoons}} Br_2^- + Br^-.$$

Fig. 2. Size dependence of the mean walklength for flip processes on a periodic square planar lattice. The curve with gray circles corresponds to an estimate of the walklength $\langle n \rangle_{est} = 1/\lambda$ obtained from the solution of the eigenvalue Eq. (11) in the framework of the kinetic model, whereas the curve with gray triangles corresponds to the mean walklength $\langle n \rangle_{calcd}$ calculated from a discrete Markovian model (fundamental matrix approach used in Ref. [2]) and confirmed by Monte Carlo simulations. The red curve corresponds to a Monte Carlo simulation where a spin flip occurs in the course of the random walk. The lines between the different symbols are simply guides to the eye. (For interpretation of the references to colour in this figure legend and in the text, the reader is referred to the web version of this article.)

In what follows, we shall focus on the second reaction of scheme (12), namely the dismutation reaction. Analysis of the experimental pulse radiolysis data using methods developed earlier [23–28] led to the conclusion that the reaction proceeds via two kinetic processes with Br_2^- radicals involved: a fast first-order process driven by $d = 2$ (surface) diffusion and a slow second-order process involving $d = 3$ diffusion. The $d = 2$ process takes place via a single pathway (designated a below), namely *intra*micellar surface diffusion. The $d = 3$ reaction process involves two different pathways, an *inter*micellar reaction (pathway b) and bulk reaction in the aqueous phase (pathway c). The experimental values for the $d = 2$ and the $d = 3$ processes reported in Ref. [1] are, respectively, $k_2 = 2.1 \times 10^6 \text{ s}^{-1}$ and $k_3 = 1.46 \times 10^9 \text{ M}^{-1}\text{s}^{-1}$.

To provide a theoretical basis for understanding these results, the study [1] drew upon analytic results derived by Montroll [10]. In a seminal contribution, Montroll considered (certain) d-dimensional Euclidean lattices subject to periodic boundary conditions, and developed asymptotic expressions for the number of displacements $\langle n \rangle$ of a random walker before "trapping" at a *stationary* target site. By making reasonable estimates of the number N of sites available to a diffusing Br_2^- species on a CTAB micellar surface (viz., $N = 55$), and using concentration arguments to design a companion $d = 3$ lattice, an expression was derived (see Appendix)

$$k_2(a)/[2k_3(b + c)] = \ln(2)[Br_2^-]_0 \langle n \rangle_3 / \langle n \rangle_2 \tag{13}$$

relating the ratio of rate constants $k_2(a)$ and $2k_3(b + c)$ to the mean walklength in dimensions $d = 2$ and $d = 3$, $\langle n \rangle_2$ and $\langle n \rangle_3$, of a diffusing Br_2^- radical before an irreversible reaction with a second, *stationary* Br_2^- radical ion occurred. The value $[Br_2^-]_0$ of the initial concentration of Br_2^- at time $t = 0$, 2.69×10^{-5} M was obtained from experimental data [1].

The value of $k_2(a)/[2k_3(b + c)]$ reported in Ref. [1] based on Montroll's asymptotic results was (in M units)

$$(k_2/2k_3)_{MONTROLL} = 7.7 \times 10^{-3}$$

which was compared with the experimental value of the ratio

$$(k_2/2k_3)_{EXP} = 2.1 \times 10^6/(1.46 \times 10^9) = 1.5 \times 10^{-3}.$$

In 1982 den Hollander and Kasteleyn [29] re-derived an expression for $\langle n \rangle_2$ for square planar lattices and found a discrepancy between their theoretical result and that of Montroll. They traced the discrepancy to one of the coefficients in Montroll's asymptotic expansion. Subsequently it was found that if the corrected (den Hollander–Kasteleyn) coefficient was incorporated into Montroll's theory, agreement between theory and numerical experiment was essentially exact [30]. If one uses the corrected Montroll expression to calculate the mean walklength for the same number $N(=55)$ of sites estimated in Ref. [1], one finds $\langle n \rangle_2 \sim 64.7$. Using this value in (6), a revised estimate for $k_2(a)/[2k_3(b + c)]$ can be obtained:

$$(k_2/2k_3)_{H-K} = 9.7 \times 10^{-3},$$

a value which is (still) within a factor of ten of the experimentally determined value of the ratio $(k_2/2k_3)_{EXP}$.

3.2. Extension to the asynchronous case on a cubic shell

As noted above, the analytic results that were available at the time that [1] was written were principally those derived by Montroll, Weiss and coworkers (see, for example, Ref. [21]). Since then, there has been an extensive development of

Table 1
Experimental and theoretical values for the ratio of kinetic constants characterizing the $d = 2$ and the $d = 3$ processes.

$(k_2/2k_3)_{EXP}$	$(k_2/2k_3)_{MONTROLL}$	$(k_2/2k_3)_{H\text{-}K}$	$(k_2/2k_3)_{C\text{-}SYN}$	$(k_2/2k_3)_{C\text{-}ASY}$
1.5×10^{-3}	7.7×10^{-3}	9.7×10^{-3}	7.2×10^{-3}	6.9×10^{-3}

the theory of diffusion-controlled reactive processes in compartmentalized systems [31]. Moreover, analytical methods for analyzing synchronous vs. asynchronous lattice dynamics are now available [11–13]. Accordingly, it is of interest to explore how the dismutation analysis would change if two of the assumptions made in analyzing the *intra* micellar process (above) were relaxed.

First, although the surface of a zeolite crystal might be of spatial extent large enough to warrant the adoption of a planar lattice model, such a model would be, at best, approximate when considering the finite, bounded surface of a CTAB micelle. The diffusion of the Br_2^- radical ions on a CTAB micelle surface is more sensibly described by a $\Omega = 2$ shell, not a $\Omega = 0$ periodic, planar surface (the designated lattice in the Montroll analysis). Secondly, given the identity of the two species involved in the dismutation reaction, two Br_2^- radical ions, there is no reason to presume that one member of the pair is permanently anchored at a target site on the surface (the Montroll scenario); both Br_2^- species can surely move independently, either synchronously or asynchronously.

At this point, one can take advantage of the lattice statistical approach described in Section 2 to translate the results obtained for a system of two radical ions with spin on a zeolite support to the case of two Br_2^- ion radicals on a micellar surface. Then, from the data depicted in Fig. 1 for the no-flip synchronous case, one can determine the value of $\langle n \rangle_2$ for two Br_2^- species moving *synchronously* on a $\Omega = 2$ (CTAB) shell characterized by nearly the same number N of available sites as estimated in Ref. [1]. For a Cartesian shell of $N = 56$ sites, the mean walklength $\langle n \rangle_2$ is calculated to be 87.1 which leads to the revised estimate

$$(k_2/2k_3)_{C\text{-}SYN} = \ln(2)[Br_2^-]\langle n \rangle_3/\langle n \rangle_2 = 7.2 \times 10^{-3}.$$

Thus, an improved representation of the micellar surface leads to a result which re-establishes the earlier, putative agreement with experiment, but one can go further. If one recognizes that, in their respective motions, the two diffusing Br_2^- ion radicals encounter fluxional imperfections on the CTAB surface owing to the dynamic nature of micelle geometry, it is far more likely that the two species will migrate *asynchronously* on the micelle surface. In this case, the value of the mean walklength is somewhat larger, $\langle n \rangle_2 = 92.1$. Thus,

$$(k_2/2k_3)_{C\text{-}ASY} = \ln(2)[Br_2^-]\langle n \rangle_3/\langle n \rangle_2 = 6.9 \times 10^{-3},$$

and the agreement between experiment and theory is further enhanced.

As a summary of the results in this section, Table 1 shows the kinetic constant ratios

$$(k_2/2k_3)_{EXP}, \quad (k_2/2k_3)_{MONTROLL}, \quad (k_2/2k_3)_{H\text{-}K}, \quad (k_2/2k_3)_{C\text{-}SYN} \text{ and } (k_2/2k_3)_{C\text{-}ASY},$$

respectively obtained from the experiment, from Montroll's original theory for asynchronous motion on a periodic square planar lattice, from the improved theory by den Hollander and Kasteleyn (HK) for asynchronous motion on a periodic square planar lattice, from the extended theory for synchronous motion on the surface of a cube and from the extended theory for asynchronous motion on the surface of a cube. As noted above, the latter estimate $(k_2/2k_3)_{C\text{-}ASY}$ is the one in closest agreement with the experimental value. Although still "off" by a factor of four, the result is surprisingly good, given the simplicity of the Markovian description.

4. Discussion

The conclusions reached in this study follow directly from the results presented in the previous two sections. We have considered a generalization of diffusion–reaction theory in which the random motion of two reactants is either fully synchronous or fully asynchronous, and studied the dynamical consequences in two experimental systems: the CTAB/Br_2^- system and that of triplet geminate pairs on a zeolite.

In this more general setting, we were able to show quantitatively that the main result reported in Ref. [1] stands, viz., the CTAB/Br_2^- system provides the first example of an experimental system in which two kinetic components of a diffusion-controlled reaction differing in the dimensionality of the reaction space [3] could be clearly distinguished and quantified. With respect to the study of triplet geminate pairs on a zeolite, a deeper understanding of the results presented in Ref. [2] emerged.

In these studies, a range of interesting conceptual issues arose, which we shall now elaborate. Beyond the fact that asynchronous dynamics may arise as a result of disorder (i.e., geometric imperfections) in the system, these two extreme cases were purposefully chosen so as to provide the strongest possible contrast and thereby facilitate the investigation of effects due to changes in the position update rules. However, there can be instances where a combination of synchronous and asynchronous motion may determine the kinetics of a chemical rate process. For example, in the geminate pair problem, some regions of the zeolite surface will be spatially uniform, whereas other regions may have imperfections. To the extent

that the motion of a diffusing species is compromised by the presence of local imperfections, asynchronous motion of the two reactants may dominate the kinetics. In studies carried out on different zeolite surfaces, it may be possible to gauge the relative homogeneity of different surfaces in a time-resolved experiment.

From our results, we have concluded that synchronous transport leads to the more efficient reactive encounters. However, if the reactants are localized in a "cage" environment, synchronous displacements might also enhance the escape probability of reactants from the "cage". In this case, the effective cross section of the reaction may *decrease*, an effect which can become dominant when the number N of lattice sites is decreased or when the dimensionality of the system is increased for fixed N. For systems of finite size, the overall statistical behavior of the system can thus be a trade-off between diffusion-facilitated reactive encounters and an effective decrease in cross section with increasing synchronicity.

The counterintuitive effect noted in the preceding paragraph is reminiscent of evidence reported previously by Turro, et al. [32] in their experimental study of recombination reactions of triplet geminate pairs. For the case where the geminate pairs are strictly confined to "supercages", these authors found "normal" and "inverted" regions of recombination probability, noting that the probability of recombination can decrease as the size of the supercage decreases and the frequency of reencounters increases. Specifically, for their system of geminate pairs sequestered in a micelle, they predicted that in appropriate situations, "the rate of spin-selective reactions in micellized pairs will be decelerated if the encounter frequency properly couples with the electron spin exchange".

In terms of the theory of finite Markov processes, the above effect can be described as follows. If P_1 and P_2 are the respective single-step probabilities for X_1 and X_2, the walklength $\langle n \rangle$ may not necessarily be a simple function of the joint probability $P_S = P_1 P_2$ for a synchronous event; there may be regions of parameter space where $\langle n \rangle$ *increases* with increasing P_S. To be precise, the Markovian theory and supporting lattice Monte Carlo calculations reported in Ref. [13] documented that, whereas P_S is expected to increase with increasing temperature, constraints imposed *solely* by geometrical confinement of reactants can lead to a situation where the reaction efficiency *decreases* with *increase* in temperature.

In analogy with Marcus' theory for electron transfer reactions and Turro et al.'s model for geminate recombination reactions, such regions were also termed "inverted regions". However, as stressed above, this Markovian inversion scenario is a sole consequence of classical *geometrical* constraints imposed on the system, in contrast to the "inverted regions" associated with the quantum-mechanical electron transfer theory of Marcus [33–37] and the electron spin exchange model of Turro et al. [32].

To summarize, we have demonstrated that diffusion-controlled reactive processes in which the reactants move synchronously both on a periodic planar lattice and a bounded surface of a cube are more efficient than if their joint displacements are asynchronous. And, secondly, we have documented that reactive processes taking place on surfaces of the same topological dimension but having different Euler characteristics, here planar periodic lattices (topologically equivalent to a torus) and finite bounded surfaces (Cartesian shells), can be discriminated, with the efficiency higher on $\Omega = 0$ surfaces. We believe these conclusions are relevant not only to the systems studied here, but also to a wide class of diffusion-controlled reactive processes in/on compartmentalized systems [31].

Although we now have a better understanding of the role of different surface topologies in influencing the kinetics, the zeolite surface was (still) modeled as a homogeneous lattice, one free of defects and/or imperfections such as steps, ledges and kinks. As noted by a referee (see Section 2), the description of radical decay kinetics on an irregular (random) surface would lead to a more realistic description of the underlying diffusion–reaction process. In fact, more detailed modeling would also have immediate relevance to experimental studies of "kinetic roughening" in the nucleation of zeolite crystallites such as silicalite -1 [38] and proteins [39] such as glucose isomerase [40], and to related theoretical studies [41,42].

As regards the dismutation reaction, since both Br_2^- and the micellar CTAB head groups are charged, a systematic study of Coulombic effects in influencing intramicellar vs. intermicellar diffusion–reaction kinetics would be of interest. One anticipates that down-range attractive interactions will affect, perhaps dramatically, results obtained when only nearest-neighbor steric effects are considered (as here). Although the separation of time scales found experimentally in the dismutation reaction suggested the possible relevance of *reduction of dimensionality*, introduced by Adam and Delbruck decades ago, the importance of this effect when long-range forces are at play has not been documented, so results obtained when the above program is carried out would be instructive.

Lastly, we did not consider density effects at fixed system size. Whereas asymptotic estimates for the asynchronous case [17] show that increasing the number of reactants at a fixed system size leads to a drastic reduction in the mean encounter time, estimates similar to Montroll's are not available for the synchronous case. As this comment and those in the preceding paragraphs have made clear, there is much that needs to be done to broaden the generality of the approach taken here. However, we now have the advantage that theoretical and computational methods developed extensively in recent years can be used to revisit two, different, experimental realizations of surface-mediated, radical decay reactions [1,2] for which the importance of geometrical factors has been demonstrated.

Acknowledgements

Appendix. Derivation of Eq. (13)

Eq. (13) was obtained assuming that the distance d_i between adjacent lattice sites and the "hopping" velocity v_i of Br_2^- were the same on both $d = 2$ and $d = 3$ lattices, so that the ratio of the times $\langle \tau \rangle_2$ and $\langle \tau \rangle_3$ scaled as $\langle n \rangle_2$ and $\langle n \rangle_3$. This ratio can then be related to the half-lives of the dismutation reactions, and from thence to the respective rate constants; see Ref. [43]. For the first-order process on $d = 2$ [the intramicellar reaction (a)],

$$\langle \tau \rangle_2 = (\ln 2)/k(a)$$

and for the *two* second-order pathways in $d = 3$ [the inter-micellar reaction (b) and/or the micellar-bulk reaction (c)]

$$\langle \tau \rangle_3 = 1/(2k_3(b + c)[Br_2^-]_0).$$

Then,

$$\langle n \rangle_2 / \langle n \rangle_3 = [(\ln 2)/k(a)]/[1/(2k_3(b + c)[Br_2^-]_0)]$$

from which Eq. (13) follows.

References

[1] A.J. Frank, M. Grätzel, John J. Kozak, J. Am. Chem. Soc. 98 (1976) 3317–3321.
[2] John J. Kozak, C. Nicolis, G. Nicolis, Nicolas J. Turro, J. Phys. Chem. A 105 (2001) 10949–10951.
[3] G. Adam, M. Delbruck, in: A. Rich, W. Davidson (Eds.), Structural Chemistry and Molecular Biology, W.H. Freeman, San Francisco, CA, 1968.
[4] M. Bramson, J.L. Lebowitz, Phys. Rev. Lett. 61 (1988) 2397–2400.
[5] A. Szabo, R. Zwanzig, N. Agmon, Phys. Rev. Lett. 61 (1999) 2496–2499.
[6] A.J. Bray, R.A. Blythe, Phys. Rev. Lett. 89 (2002) 150601.
[7] G. Oshanin, O. Bénichou, M. Coppey, M. Moreau, Phys. Rev. E 66 (2002) 060101.
[8] M. Moreau, G. Oshanin, O. Bénichou, M. Coppey, Phys. Rev. E 67 (2003) 045104.
[9] M. Moreau, G. Oshanin, O. Bénichou, M. Coppey, Physica A 327 (2003) 99–104.
[10] E.W. Montroll, J. Math. Phys. 10 (1969) 753–765.
[11] J.J. Kozak, G. Nicolis, C. Nicolis, J. Chem. Phys. 113 (2000) 8168–8174.
[12] E. Abad, G. Nicolis, Jonathan L. Bentz, John J. Kozak, Physica A 326 (2003) 69–87.
[13] E. Abad, John J. Kozak, Physica A 370 (2006) 501–524.
[14] N.J. Turro, B. Kraeutler, Acc. Chem. Res. 13 (1980) 369–377;
     N.J. Turro, A.L. Buchachenko, V.F. Tarasov, Acc. Chem. Res. 28 (1995) 69–80;
     N.J. Turro, Acc. Chem. Res. 33 (2000) 637–646.
[15] N.J. Turro, Z. Zhang, Tetrahedron Lett. 29 (1989) 3761–3764.
[16] E.N. Step, A.L. Buchachenko, N.J. Turro, J. Am. Chem. Soc. 116 (1992) 5462–5466.
[17] A.L. Buchachenko, V.L. Berdinsky, J. Phys. Chem. 100 (1996) 18292–18299.
[18] V. Ramamurthy, J.V. Caspar, D.F. Eaton, E.W. Kuo, D.R. Corbin, J. Am. Chem. Soc. 114 (1992) 3882–3892.
[19] S. Uppili, V. Marti, A. Nikolaus, S. Jockusch, W. Adam, P.S. Engel, N.J. Turro, V. Ramamurthy, J. Am. Chem. Soc. 122 (2000) 11025–11026.
[20] E.N. Step, A.L. Buchachenko, N.J. Turro, J. Am. Chem. Soc. 116 (1994) 5462–5466.
[21] G.H. Weiss, Aspects and Applications of the Random Walk, North Holland, Amsterdam, 1994.
[22] H. Scher, M. Lax, Phys. Rev. B 7 (1973) 4492–4502;
     H. Scher, M. Lax, Phys. Rev. B 7 (1973) 4502–4519.
[23] E.H. Cordes, Reaction Kinetics in Micelles, Plenum Publishing Co., New York, 1973.
[24] C. Tanford, The Hydrophobic Effect, Formation of Micellar and Biological Membranes, Wiley-Interscience, New York, 1973.
[25] M. Grätzel, A. Henglein, E. Janata, Ber. Bunsenges. Phys. Chem. 79 (1975) 475–480.
[26] A. Henglein, W. Schnabel, J. Wendenburg, Einführung in die Strahlenchemie, Verlag Chemie, Weinheim, Bergstr., Germany, 1969;
     B. Cercek, M. Ebert, C.W. Gilbert, A.J. Swallow, in: M. Ebert, J.P. Keene, A.J. Swallow, J.H. Baxendale (Eds.), Pulse Radiolysis, Academic Press, New York, 1965, p. 83;
     H.C. Sutton, G.E. Adams, J.W. Boag, B.D. Michael, in: M. Ebert, J.P. Keene, A.J. Swallow, J.H. Baxendale (Eds.), Pulse Radiolysis, Academic Press, New York, 1965, p. 61.
[27] L.I. Grossweiner, M.S. Matheson, J. Phys. Chem. 61 (1957) 1089–1095;
     L.M. Dorfman, L.A. Taub, R.E. Buhler, J. Chem. Phys. 36 (1962) 3051–3061;
     B. Cereck, M. Ebert, J.P. Keene, A.J. Swallow, Science 145 (1964) 919–920;
     M.S. Matheson, W.A. Mulac, J.L. Weeks, J. Rabani, J. Phys. Chem. 70 (1966) 2092–2099;
     D. Zehavi, J. Rabani, J. Phys. Chem. 76 (1972) 312–319.
[28] P.H. Elworthy, A.T. Florence, C.B. MacFarlane, Solubilization by Surface-Active Agents, Chapman and Hall, London, 1968;
     K. Shinoda, in: E.M. Loebel (Ed.), Colloidal Surfactants, Academic Press, New York, 1963.
[29] W.Th.F. den Hollander, P.W. Kasteleyn, Physica A 112 (1982) 523–543.
[30] Philip A. Politowicz, John J. Kozak, Langmuir 4 (1988) 305–320.
[31] J.J. Kozak, Adv. Chem. Phys. 115 (2000) 245–406.
[32] N.J. Turro, A.L. Buchachenko, V.F. Tarasov, Acc. Chem. Res. 28 (1995) 69–80.
[33] R.A. Marcus, J. Chem. Phys. 24 (1956) 966–978.
[34] R.A. Marcus, N. Sutin, Biochim. Biophys. Acta 811 (1985) 265–322.
[35] R.A. Marcus, Adv. Chem. Phys. 106 (1999) 1–6.
[36] H.B. Gray, J.R. Winkler, Quart. Rev. Biophys. 36 (2003) 341–372.
[37] H.B. Gray, J.R. Winkler, Proc. Natl. Acad. Sci. USA 102 (2005) 3534–3539.
[38] S. Kremer, C. Kirschhock, A. Aerts, K. Villani, J. Martens, O. Levedev, G. Van Tendeloo, Adv. Mater. (Weinheim, Ger.) 15 (2003) 1705–1707;
     C. Kirschhock, S. Kremer, J. Vermant, G. Van Tendeloo, P.A. Jacobs, J. Martens, Chem. Eur. J. 11 (2005) 4306–4313.
[39] K. Chen, P.G. Vekilov, Phys. Rev. E 66 (2000) 021606;
     P.G. Vekilov, J.I. Alexander, Chem. Rev. 100 (2000) 2061–2090.
[40] M. Sleutel, C. Vandee, C.V. de Weerdt, K. Deconniere, D. Maews, L. Wyns, R. Willaert, Cryst. Growth Des. 8 (2008) 1173–1180;
     M. Sleutel, R. Willaert, C. Evard, L. Wyns, D. Maes, Cryst. Growth Des. 9 (2009) 497–504.
[41] Y. Saito, Statistical Physics of Crystal Growth, World Scientific, Singapore, 1996.
[42] R.A. Garza Lopez, P. Bouchard, G. Nicolis, M. Sleutel, J. Brzezinski, J.J. Kozak, J. Chem. Phys. 128 (2008) 114701;
     J.F. Lutsko, V. Basios, G. Nicolis, J.J. Kozak, M. Sleutel, D. Maes, J. Chem. Phys. 132 (2010) 035102.
[43] W.J. Moore, Physical Chemistry, 3rd ed., Prentice-Hall Inc., Englewood Cliffs, NJ, 1962, pp. 260–263.